

Cite this: *Phys. Chem. Chem. Phys.*, 2012, **14**, 14769–14774

www.rsc.org/pccp

PAPER

## Double-chain planar $D_{2h}$ $B_4H_2$ , $C_{2h}$ $B_8H_2$ , and $C_{2h}$ $B_{12}H_2$ : conjugated aromatic borenes†

Da-Zhi Li,<sup>ab</sup> Qiang Chen,<sup>ac</sup> Yan-Bo Wu,<sup>a</sup> Hai-Gang Lu<sup>a</sup> and Si-Dian Li<sup>\*ac</sup>

Received 21st March 2012, Accepted 17th May 2012

DOI: 10.1039/c2cp40902j

Based upon comprehensive theoretical investigations and known experimental observations, we predict the existence of the double-chain planar  $D_{2h}$   $B_4H_2$ (**1**),  $C_{2h}$   $B_8H_2$ (**3**), and  $C_{2h}$   $B_{12}H_2$ (**5**) which appear to be the lowest-lying isomers of the systems at the density functional theory level. These conjugated aromatic borenes turn out to be the boron hydride analogues of the conjugated ethylene  $D_{2h}$   $C_2H_4$ (**2**), 1,3-butadiene  $C_{2h}$   $C_4H_6$ (**4**), and 1,3,5-hexatriene  $C_{2h}$   $C_6H_8$ (**6**), respectively, indicating that a  $B_4$  rhombus in  $B_{2n}H_2$  borenes ( $n = 2, 4, 6$ ) is equivalent to a C=C double bond unit in the corresponding  $C_nH_{n+2}$  hydrocarbons. Detailed canonical molecular orbital (CMO), adaptive natural density partitioning (AdNDP), and electron localization function (ELF) analyses unravel the bonding patterns of these novel borene clusters and indicate that they are all overall aromatic in nature with the formation of islands of both  $\sigma$ - and  $\pi$ -aromaticity. The double-chain planar or quasi-planar  $C_{2v}$   $B_3H_2^-$ (**7**),  $C_2$   $B_5H_2^-$ (**8**), and  $C_{2h}$   $B_6H_2$ (**9**) with one delocalized  $\pi$  orbital,  $C_{2v}$   $B_7H_2^-$ (**10**),  $C_2$   $B_9H_2^-$ (**11**), and  $C_{2h}$   $B_{10}H_2$ (**12**) with two delocalized  $\pi$  orbitals, and  $C_{2v}$   $B_{11}H_2^-$ (**13**) with three delocalized  $\pi$  orbitals are found to be analogous in  $\pi$ -bonding to  $D_{2h}$   $B_4H_2$ (**1**),  $C_{2h}$   $B_8H_2$ (**3**), and  $C_{2h}$   $B_{12}H_2$ (**5**), respectively. We also calculated the electron affinities and ionization potentials of the neutrals and simulated the photoelectron spectroscopic spectra of the monoanions to facilitate their future experimental characterization. The results obtained in this work enrich the analogous relationship between hydroborons and their hydrocarbon counterparts and help to understand the high stability of the theoretically predicted all-boron nanostructures which favor the formation of double-chain substructures.

### I. Introduction

As the prototype of electron deficient elements in the periodic table, boron has a rich chemistry next only to carbon. Boron hydrides  $B_nH_m$  have attracted huge attention in both chemistry and materials sciences, with examples including  $B_2H_4$ ,<sup>1</sup>  $BH_3$ ,  $B_2H_6$ ,  $B_3H_7$ ,  $B_4H_{10}$ ,  $B_5H_9$  and  $B_5H_{11}$ ,<sup>2</sup>  $B_nH^+$  ( $n = 1-13$ ),<sup>3</sup>  $B_2H^+$ ,  $B_2H_2^+$ , and  $B_3H_2^+$ ,<sup>4</sup>  $B_2H_{2n}^{2+}$  dications ( $n = 1-4$ ),<sup>5</sup>  $B_nH_n$  neutrals ( $n = 5-13, 16, 19, 22$ ) and more typically, the cage-like  $B_nH_n^{-2-}$  dianions ( $n = 5-13$ ).<sup>6-8</sup> Detailed theoretical investigations on a series of small hydrogen-rich boron hydride clusters with less than four boron atoms have also been reported recently.<sup>9</sup> However, relatively little is known about the nature of boron-rich

$B_nH_m$  clusters which contain fewer hydrogen atoms than boron ( $n > m$ ). A few previously reported examples include the perfectly planar  $C_{2v}$   $B_7H_2^-$  which is fundamentally different from bare  $C_{6v}$   $B_7^-$ ,<sup>10,11</sup> the perfectly planar  $D_{3h}$   $B_{12}H_6$  (the so called borozene) which is the boron hydride analogue of benzene,<sup>12</sup> the perfectly planar concentric  $\pi$ -aromatic  $D_{3h}$   $B_{18}H_3^-$ ,  $D_{2h}$   $B_{18}H_4$ ,  $C_{2v}$   $B_{18}H_5^+$ , and  $D_{6h}$   $B_{18}H_6^{2+}$  (the so called borannulenes) which are analogous to [10]annulene  $D_{10h}$   $C_{10}H_{10}$  (but fundamentally different from bare  $C_{3v}$   $B_{18}$ ),<sup>13</sup> and the perfectly planar  $C_{3h}$   $B_6H_3^+$  and  $C_{2h}$   $B_8H_2$  which are the inorganic analogues of cyclopropene cation  $D_{3h}$   $C_3H_3^+$  and cyclobutadiene  $D_{2h}$   $C_4H_4$  (but much different from  $C_{2h}$   $B_6$  and  $D_{7h}$   $B_8$ , respectively).<sup>14</sup> Planar boron-rich boron hydride clusters also include  $B_4H_n$  ( $n = 1-3$ )<sup>15</sup> and  $B_{16}H_n$  ( $n = 1-6$ ).<sup>16</sup> Our group recently reported a systematic investigation on the effect of hydrogenation of  $B_{12}^{0/-}$  and found that there exists a 2D–3D transition between  $n = 3-4$  in  $B_{12}H_n^{0/-}$  ( $n = 1-6$ ).<sup>17</sup> The available results indicate that partial hydrogenation leads to planarization in small boron-rich  $B_nH_m$  clusters (but may cause dramatic changes to the  $B_n$  cores) and there seems to exist an interesting analogous relationship to be fully explored between planar hydroboron clusters and their hydrocarbon counterparts.<sup>12-17</sup>

<sup>a</sup> Institute of Molecular Science, the Key Laboratory of Chemical Biology and Molecular Engineering of Education Ministry, Shanxi University, Taiyuan 030006, Shanxi, People's Republic of China

<sup>b</sup> Department of Chemistry and Chemical Engineering, Binzhou University, Binzhou 256603, Shandong, People's Republic of China

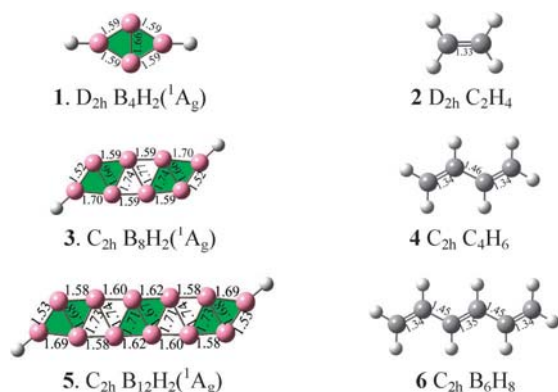
<sup>c</sup> Institute of Materials Science, Xinzhou Teachers' University, Xinzhou 034000, Shanxi, People's Republic of China.  
E-mail: lisidian@sxu.edu.cn, lisidian@yahoo.com

† Electronic supplementary information (ESI) available. See DOI: 10.1039/c2cp40902j

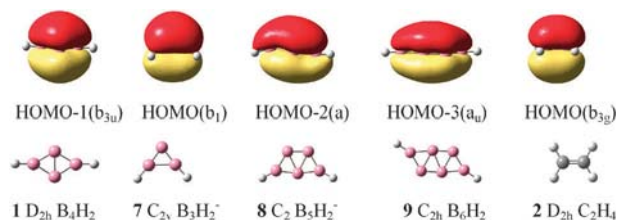
We perform in this work a systematic first-principles investigation on small boron-rich boron hydride clusters including  $B_nH_2$  neutrals ( $n = 4, 6, 8, 10, 12$ ) and  $B_nH_2^-$  monoanions ( $n = 3, 5, 7, 9, 11$ ) to enrich the analogous relationship between hydroboron clusters and their hydrocarbon counterparts. Extensive theoretical investigations indicate that double-chain (DC) planar  $D_{2h}$   $B_4H_2$ (1),  $C_{2h}$   $B_8H_2$ (3), and  $C_{2h}$   $B_{12}H_2$ (5) are the lowest-lying isomers of the systems at density functional theory (DFT) which turn out to be the borene analogues of ethylene  $C_2H_4$ (2), 1,3-butadiene  $C_4H_6$ (4), and 1,3,5-hexatriene  $C_6H_8$ (6) in both geometrical and electronic structures, respectively, establishing an interestingly analogous relationship between the  $B_{2n}H_2$  clusters ( $n = 2, 4, 6$ ) and their conjugated hydrocarbon counterparts  $C_nH_{n+2}$ . Detailed canonical molecular orbital (CMO), adaptive natural density partitioning (AdNDP),<sup>18</sup> electron localization function (ELF),<sup>19</sup> and nucleus-independent chemical shift (NICS)<sup>20</sup> analyses are performed to analyze the bonding patterns and aromaticity of these DC planar clusters. Electron affinities and ionization potentials of the neutrals and photoelectron spectroscopy (PES) spectra of the monoanions are calculated to facilitate their future experimental syntheses and characterizations. The results obtained in this work have important implications in understanding the high stability of the theoretically predicted double-ring tubular  $B_{20}$ ,<sup>21</sup> cage-like  $B_{80}$ ,<sup>22</sup> and 2D DC-interwoven boron  $\alpha$ -sheet<sup>23</sup> which all favor the formation of double-chain substructures.

## II. Computational procedures

Structural optimizations and frequency analyses were carried out using the DFT-B3LYP method<sup>24,25</sup> with the base set of 6-311+g(d,p) implemented in the Gaussian 03 program.<sup>26</sup> Initial structures were constructed based upon the low-lying isomers of the bare  $B_n^{0/-}$  clusters ( $n = 3-12$ )<sup>21</sup> by adding two terminal hydrogen atoms at the corner positions. More extensive global minimum searches were performed using the gradient embedded genetic algorithm (GEGA).<sup>27,28</sup> Relative energies for important low-lying isomers are further refined using the coupled cluster method with triple excitations (CCSD(T))<sup>29</sup> at the B3LYP geometries. Fig. 1 compares the optimized structures of  $D_{2h}$   $B_4H_2$ (1),  $C_{2h}$   $B_8H_2$ (3), and  $C_{2h}$   $B_{12}H_2$ (5) at B3LYP/6-311+g(d,p) compared with that of ethylene  $D_{2h}$   $C_2H_4$ (2),  $C_{2h}$   $C_4H_6$ (4), and  $C_{2h}$   $C_6H_8$ (6). Fig. 2 shows the



**Fig. 1** Optimized structures of  $D_{2h}$   $B_4H_2$ (1),  $C_{2h}$   $B_8H_2$ (3), and  $C_{2h}$   $B_{12}H_2$ (5) at B3LYP/6-311+g(d,p) compared with that of ethylene  $D_{2h}$   $C_2H_4$ (2), 1,3-butadiene  $C_{2h}$   $C_4H_6$ (4), and 1,3,5-hexatriene  $C_{2h}$   $C_6H_8$ (6).



**Fig. 2**  $\pi$ -CMOs of the optimized  $D_{2h}$   $B_4H_2$ (1),  $C_{2v}$   $B_3H_2^-$ (7),  $C_2$   $B_5H_2^-$ (8), and  $C_{2h}$   $B_6H_2$ (9) compared with that of ethylene  $D_{2h}$   $C_2H_4$ (2).

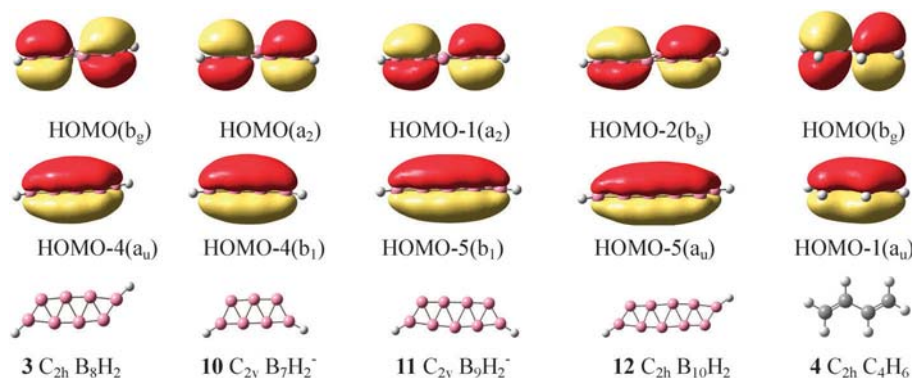
occupied  $\pi$ -CMOs of  $D_{2h}$   $B_4H_2$ (1),  $C_{2v}$   $B_3H_2^-$ (7),  $C_2$   $B_5H_2^-$ (8), and  $C_{2h}$   $B_6H_2$ (9) compared with that of  $D_{2h}$   $C_2H_4$ (2). The occupied  $\pi$ -CMOs of  $C_{2h}$   $B_8H_2$ (3),  $C_{2v}$   $B_7H_2^-$ (10),  $C_2$   $B_9H_2^-$ (11), and  $C_{2h}$   $B_{10}H_2$ (12) are depicted in Fig. 3 compared with that of  $C_{2h}$   $C_4H_6$ (4). Fig. 4 exhibits the occupied  $\pi$  CMOs of  $C_{2h}$   $B_{12}H_2$ (5) and  $C_{2v}$   $B_{11}H_2^-$ (13) compared with that of  $C_{2h}$   $C_6H_8$ (6). Alternative low-lying isomers of  $B_nH_2$  neutrals ( $n = 4, 6, 10, 12$ ) and  $B_nH_2^-$  monoanions ( $n = 3, 5, 9, 11$ ) are summarized in Fig. 1S in the ESI.† Detailed AdNDP,<sup>18</sup> ELF,<sup>19,30</sup> and NICS<sup>20</sup> analyses were performed to analyze the bonding patterns and aromaticity of the concerned systems. The separated  $ELF_\sigma$  and  $ELF_\pi$  bifurcation values were approximated using the Molekel 5.4 software<sup>31</sup> and the dissected contributions NICS $_\sigma$  and NICS $_{\pi-zz}$  from  $\sigma$  and  $\pi$  molecular orbitals (MOs) to total NICS<sup>20</sup> were computed at the rhombus centers using the NBO5.0 program.<sup>32</sup> Table 1 compares the  $\sigma$  and  $\pi$ -bonding patterns of  $D_{2h}$   $B_4H_2$ ,  $C_{2h}$   $B_8H_2$ , and  $C_{2h}$   $B_{12}H_2$  at both ELF and AdNDP based on B3LYP densities, with the bifurcation values of  $ELF_\sigma$ ,  $ELF_\pi$ , and their averages  $ELF_{av}$  ( $ELF_{av} = (ELF_\sigma + ELF_\pi)/2$ ) and the dissected NICS values of NICS $_\sigma$  and NICS $_{\pi-zz}$  indicated. Fig. 5 shows the simulated PES spectra of the  $B_nH_2^-$  monoanions ( $n = 3-9$  and 11) using the time-dependent DFT (TDDFT) method<sup>33</sup> to facilitate their future PES characterizations.

## III. Results and discussions

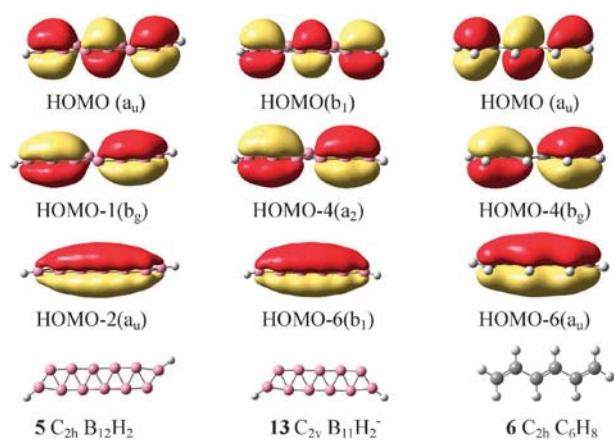
### 1 Structures and orbital analyses

We start from  $D_{2h}$   $B_4H_2$ (1), the smallest neutral borene cluster studied in this work. As clearly shown in Fig. 1 and Fig. 1S,† the ground state of  $B_4H_2$ ( $^1A_g$ ) possesses a  $D_{2h}$  rhombus structure with the short diagonal B–B bond length of 1.66 Å and peripheral B–B distance of 1.59 Å which lies 0.71 eV and 0.57 eV lower than the second lowest-lying isomer of  $C_s$   $B_4H_2$  at B3LYP and CCSD(T), respectively.  $D_{2h}$   $B_4H_2$ (1) can be obtained by attaching two –H terminals to the rhombus ground state of  $D_{2h}$   $B_4^{2+}$  along the long diagonal. We also notice that the rhombus structure of  $D_{2h}$   $B_4H_2$ (1) is well maintained in its anion  $D_{2h}$   $B_4H_2^-$ . Interestingly, the delocalized  $4c-2e$   $\pi$ -HOMO-1( $b_{3u}$ ) of  $D_{2h}$   $B_4H_2$ (1) can be traced back to the delocalized  $\pi$ -HOMO-1( $b_{3u}$ ) of the rhombus  $D_{2h}$   $B_4$  in origin<sup>21</sup> which appears to be similar to the  $2c-2e$   $\pi$ -HOMO ( $b_{3u}$ ) of ethylene  $D_{2h}$   $C_2H_4$ (2) (see Fig. 2).

Similar ground-state structures of  $C_{2v}$   $B_3H_2^-$ (7),  $C_2$   $B_5H_2^-$ (8), and  $C_{2h}$   $B_6H_2$ (9) in triangular motifs can also be obtained by attaching two –H terminals to two corner boron atoms of  $D_{3h}$   $B_3^-$ ,  $C_{2v}$   $B_5^-$ , and  $C_{2h}$   $B_6^{2+}$  along the long



**Fig. 3**  $\pi$ -CMOs of the optimized  $D_{2h}$   $B_8H_2$ (**3**),  $C_{2v}$   $B_7H_2^-$ (**10**),  $C_2$   $B_9H_2^-$ (**11**), and  $C_{2h}$   $B_{10}H_2$ (**12**) compared with that of 1,3-butadiene  $C_{2h}$   $C_4H_6$ (**4**).



**Fig. 4**  $\pi$ -CMOs of the optimized  $C_{2h}$   $B_{12}H_2$ (**5**) and  $C_{2v}$   $B_{11}H_2^-$ (**13**) compared with that of 1,3,5-hexatriene  $C_{2h}$   $B_6H_8$ (**6**).

molecular axes, respectively, as shown in Fig. 2. Interestingly, all these DC planar  $B_nH_2$  clusters possess one multi-centered  $nc-2e$   $\pi$ -CMO ( $n = 3, 5, 6$ ) similar to the  $4c-2e$   $\pi$ -CMO of  $D_{2h}$   $B_4H_2$ (**1**) (though they have more or less peripheral B–B  $\sigma$ -bonds than the latter). Thus,  $B_3H_2^-$ (**7**),  $D_{2h}$   $B_4H_2$ (**1**),  $B_5H_2^-$ (**8**), and  $B_6H_2$ (**9**) as a group of boron hydride clusters can all be viewed as the borane analogues of ethylene  $C_2H_4$ (**2**) in terms of  $\pi$ -bonding.

The second boron hydride neutral we are concerned with in this work is the DC planar  $C_{2h}$   $B_8H_2$ (**3**,  $^1A_g$ ) which contains two adjacent  $B_4$  rhombuses (see Fig. 1). We confirmed in a previous report<sup>14</sup> that DC planar  $C_{2h}$   $B_8H_2$ (**3**) was the ground state of the system upon a partial hydrogenation of the wheel-shaped  $D_{7h}$   $B_8$ . In this work, we continue to discuss its bonding pattern and compare it with the conjugated chain-like 1,3-butadiene  $C_{2h}$   $C_4H_6$ (**4**). We notice that the two adjacent rhombuses in  $C_{2h}$   $B_8H_2$ (**3**) are very similar to  $D_{2h}$   $B_4H_2$ (**1**) in geometrical parameters (see Fig. 1) and the DC planar structure of  $C_{2h}$   $B_8H_2$ (**3**) is well preserved in its anion  $C_{2h}$   $B_8H_2^-$ . More interestingly, the two delocalized  $\pi$ -CMOs (HOMO( $b_g$ ) and HOMO-4( $a_u$ )) of  $C_{2h}$   $B_8H_2$ (**3**) spread over the molecular plane appear to be analogous to the two  $\pi$ -CMOs (HOMO( $b_g$ ) and HOMO-1( $a_u$ )) of 1,3-butadiene  $C_{2h}$   $C_4H_6$ (**4**) (see Fig. 3). Obviously, a  $B_4$  rhombus (highlighted in green in Fig. 1) in  $C_{2h}$   $B_8H_2$ (**3**) is equivalent to a C=C double bond unit in 1,3-butadiene


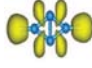
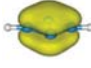
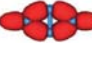
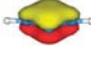
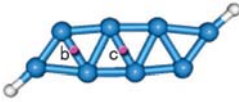

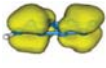
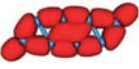
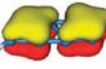
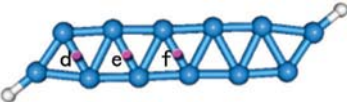
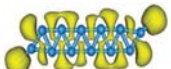
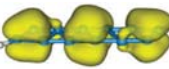
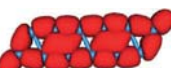
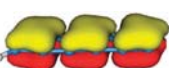
$C_{2h}$   $C_4H_6$ (**4**). Such a  $B_4$  rhombus in  $D_{2h}$   $B_4H_2$ (**1**) and  $C_{2h}$   $B_8H_2$ (**3**) consists of two edge-sharing  $B_3$  triangles with each triangle contributing one  $\pi$ -electron.

Such a  $\pi$ -MO analogy can be extended to DC planar  $C_{2v}$   $B_7H_2^-$  (**10**),  $C_2$   $B_9H_2^-$ (**11**), and  $C_{2h}$   $B_{10}H_2$ (**12**) which all possess two delocalized  $\pi$ -CMOs (see Fig. 3). It is known that a partial hydrogenation of the convex  $C_{6v}$   $B_7^-$  produces a stability conversion which leads to the formation of the DC planar  $C_{2v}$   $B_7H_2^-$ (**10**).<sup>10,11</sup> Extensive structural searches indicate that a similar stability conversion happens to the perfectly planar wheel-shaped  $D_{8h}$   $B_9^-$  upon hydrogenation to produce the ground-state structure of the DC planar  $C_2$   $B_9H_2^-$ (**11**) which follows the same structural pattern as that of  $C_{2v}$   $B_7H_2^-$ (**10**) and  $C_{2h}$   $B_8H_2$ (**3**). DC planar  $C_2$   $B_9H_2^-$ (**11**) appears to lie at least 0.40 eV and 0.34 eV lower than other low-lying isomers at B3LYP and CCSD(T), respectively (see Fig. 1S).<sup>†</sup> However, the DC planar  $C_{2h}$   $B_{10}H_2$ (**12**) neutral with one more boron atom proves to be a local minimum lying 0.49 and 0.88 eV higher than  $C_s$   $B_{10}H_2(^1A')$  at B3LYP and CCSD(T), respectively (see Fig. 1S).<sup>†</sup> Fig. 3 indicates that  $C_{2h}$   $B_8H_2$ (**3**), DC planar  $C_{2v}$   $B_7H_2^-$ (**10**),  $C_2$   $B_9H_2^-$ (**11**), and  $C_{2h}$   $B_{10}H_2$ (**12**) all possess two delocalized  $\pi$ -CMOs. They form therefore a family of borane analogues of 1,3-butadiene  $C_{2h}$   $C_4H_6$ (**4**) in  $\pi$ -bonding.

Now we turn to the DC planar  $C_{2h}$   $B_{12}H_2$ (**5**) which is the biggest and longest cluster studied in this work. It appears to be the lowest-lying isomer of the system at B3LYP (it lies at least 0.30 eV lower than other low-lying isomers at B3LYP, see Fig. 1S<sup>†</sup>). At the more accurate CCSD(T) level, this long strip-like isomer lies 0.17 eV higher than the quasi-planar  $C_1$   $B_{12}H_2(^1A)$ <sup>17</sup> which can be traced back to the ground state of the convex  $C_{3v}$   $B_{12}$ .<sup>21</sup> With such a small energy difference, the two lowest-lying isomers can be practically treated as iso-energetic species in thermodynamics. With one less boron atom than  $B_{12}H_2$ , the DC planar  $C_{2v}$   $B_{11}H_2^-$ (**13**) with a triangular motif is clearly the ground-state structure of the anion which lies at least 0.42 and 0.38 eV lower than other low-lying isomers at B3LYP and CCSD(T), respectively (see Fig. 1S<sup>†</sup>). We conclude that all the  $B_nH_2^{-/0}$  clusters in the size range between  $n = 3$ –11 possess DC planar ground-state structures except for  $n = 10$ .

As expected, the three delocalized  $\pi$ -CMOs (HOMO( $a_u$ ), HOMO-1( $b_g$ ), and HOMO-2( $a_u$ )) of  $C_{2h}$   $B_{12}H_2$ (**5**) over the molecular plane (see Fig. 4) appear to be similar to the three localized  $2c-2e$   $\pi$ -MOs (HOMO( $a_u$ ), HOMO-4( $b_g$ ), and

**Table 1** Comparison of the  $\sigma$ - and  $\pi$ -bonding patterns of  $D_{2h}$   $B_4H_2$ ,  $C_{2h}$   $B_8H_2$  and  $C_{2h}$   $B_{12}H_2$  at ELF, AdNDP, and NICS, respectively. All the AdNDP 2c–2e and 4c–2e  $\sigma$ -bonds with the occupation numbers of  $ON = 1.57\text{--}1.98 |e|$  are superimposed on one framework and all the 4c–2e  $\pi$ -bonds with  $ON = 1.79\text{--}2.00 |e|$  superimposed on another. The approximated bifurcation values of  $ELF_\sigma$ ,  $ELF_\pi$ , and their averages are also tabulated. NICS values are dissected into  $\sigma$  and  $\pi$  contributions ( $NICS(0)_\sigma$  and  $NICS(0)_{\pi_{zz}}$ ) at the centers of the symmetrically distributed  $B_4$  rhombuses

		$\sigma$	$\pi$	$ELF_{av}$
 $D_{2h}$ $B_4H_2$	ELF	 0.86	 0.99	0.93
	ADNDP			
	NICS	47.0(a)	–21.1(a)	
 $C_{2h}$ $B_8H_2$	ELF	 0.83	 0.80	0.82
	ADNDP			
	NICS	8.8(b), –6.8(c)	–22.9(b), –11.6(c)	
 $C_{2h}$ $B_{12}H_2$	ELF	 0.84	 0.62	0.73
	ADNDP			
	NICS	13.5(d), –6.0(e), –2.9(f)	–25.1(d), –11.1(e), –17.9(f)	

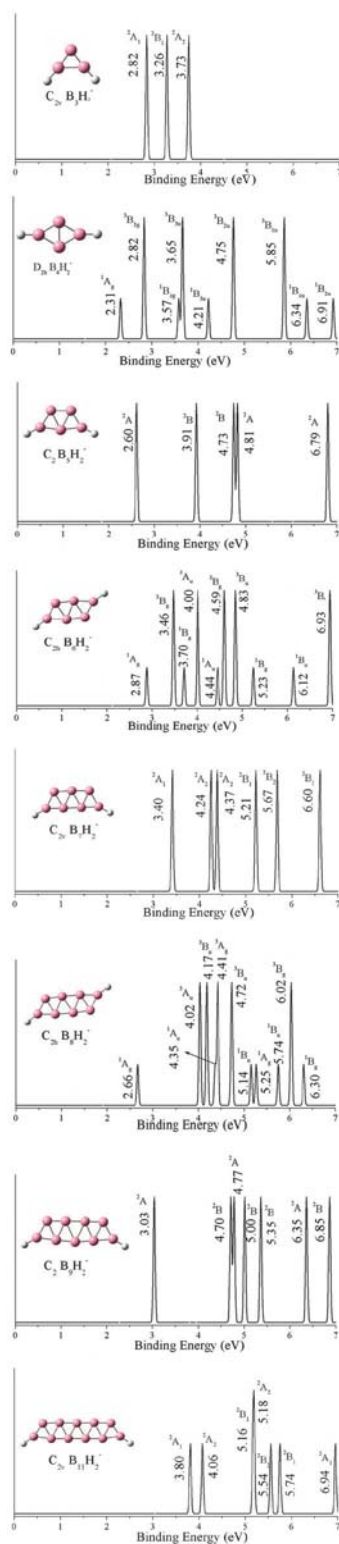
HOMO-6( $a_u$ ) of 1,3,5-hexatriene  $C_{2h}$   $C_6H_8$ (**6**).  $C_{2v}$   $B_{11}H_2^-$ (**13**) has three similar  $\pi$ -CMOs (HOMO( $b_1$ ), HOMO-4( $a_2$ ), and HOMO-6( $b_1$ )) spread over its molecular plane. Thus, both  $B_{12}H_2$ (**5**) and  $B_{11}H_2^-$ (**13**) can be viewed as boron hydride analogues of  $C_{2h}$   $C_6H_8$ (**6**) in  $\pi$ -bonding. DC planar  $B_nH_2^{-/0}$  clusters with  $n \geq 13$  turn out to be local minima of the systems which favor more spread 2D structures based upon planar or quasi-planar bare  $B_n^{-/0}$ .<sup>21</sup>

## 2 AdNDP, ELF, and NICS analyses

Detailed AdNDP and ELF analyses help to understand the bonding patterns of these DC planar borene clusters. As clearly indicated in Table 1, the AdNDP and ELF bonding patterns of neutral  $D_{2h}$   $B_4H_2$ (**1**),  $C_{2h}$   $B_8H_2$ (**3**), and  $C_{2h}$   $B_{12}H_2$ (**5**) match almost perfectly in both  $\sigma$  and  $\pi$  components which also agree well with the CMO analyses presented above.  $D_{2h}$   $B_4H_2$ (**1**) possesses two 2c–2e B–H  $\sigma$ -bonds at two ends, four peripheral 2c–2e B–B  $\sigma$ -bonds surrounding the  $B_4$  rhombus, and one totally delocalized 4c–2e  $\pi$ -bond over the molecular plane, while  $C_{2h}$   $B_8H_2$ (**3**) has two 2c–2e B–H  $\sigma$ -bonds at two ends, eight peripheral 2c–2e B–B  $\sigma$ -bonds around the DC planar  $B_8$  core, two out-of-plane 4c–2e delocalized  $\pi$ -bonds (which correspond to the sum and difference of HOMO( $b_g$ ) and HOMO-4( $a_u$ ), respectively, see Fig. 2) over two adjacent rhombuses, and one in-plane 4c–2e delocalized  $\sigma$ -bond in the central rhombus region which serves as the interval between the two 4c–2e delocalized  $\pi$  bonds, forming

an interesting conjugated delocalized  $\pi$ -bond system.  $C_{2h}$   $B_{12}H_2$ (**5**) has a similar bonding pattern: it possesses three out-of-plane 4c–2e delocalized  $\pi$ -bonds over three adjacent  $B_4$  rhombuses and two in-plane 4c–2e delocalized  $\sigma$ -bonds in two rhombus regions which serve as the intervals between the three 4c–2e delocalized  $\pi$  bonds, forming another conjugated delocalized  $\pi$ -bond system. Such conjugated delocalized  $\pi$ -bond systems in  $C_{2h}$   $B_8H_2$ (**3**) and  $C_{2h}$   $B_{12}H_2$ (**5**) appear to be similar to the conjugated localized  $\pi$ -bonding patterns in 1,3-butadiene  $C_{2h}$   $C_4H_6$ (**4**) and 1,3,5-hexatriene  $C_{2h}$   $C_6H_8$ (**6**), respectively (see Fig. 1). We also notice that, according to the AdNDP bonding patterns presented above, these conjugated neutral borenes form islands of both  $\pi$ -aromaticity (in the rhombus regions covered with 4c–2e  $\pi$  bonds) and  $\sigma$ -aromaticity (in the rhombus intervals covered with 4c–2e  $\sigma$ -bonds). Similar  $\pi$ - and  $\sigma$ -island aromaticities exist in other borene neutrals and anions studied in this work.

Santos and coworkers<sup>34</sup> have established from various organic and inorganic systems that aromatic molecules possess average bifurcation values of  $ELF_{av}$  greater than 0.70 at the interval of (0,1). In our cases, shown in Table 1,  $D_{2h}$   $B_4H_2$ (**1**),  $C_{2h}$   $B_8H_2$ (**3**), and  $C_{2h}$   $B_{12}H_2$ (**5**) possess bifurcation values of  $ELF_\sigma = 0.86, 0.83,$  and  $0.84$ ,  $ELF_\pi = 0.99, 0.80,$  and  $0.62$ , and averages of  $ELF_{av} = 0.93, 0.82,$  and  $0.73$ , respectively. These DC planar borene clusters are thus all overall aromatic in nature in ELF criteria despite their sizes and electron counts. The formation of islands of both  $\pi$  and  $\sigma$  aromaticity and the overall aromaticity



**Fig. 5** Simulated PES spectra of the ground state  $B_nH_2^-$  anions ( $n = 3-9$  and 11) at TD-B3LYP with VDE values indicated.

of these borene clusters provide extra stability to maintain the DC planar geometries of the  $B_nH_2^{-/0}$  clusters.

Detailed NICS calculations also support the formation of island aromaticities in **1**, **3**, and **5**.  $NICS(0)_{\pi_{zz}}$  is the most refined NICS index which extracts the out-of-plane tensor component of

the isotropic NICS and includes only the  $\sigma$  MO contributions for quantifying  $\sigma$ -aromaticity, while  $NICS(0)_{\sigma}$  summarizes the  $\sigma$ -MO contributions to justify the  $\sigma$ -aromaticity.<sup>20</sup> As shown in Table 1, all the  $B_4$  rhombuses covered by delocalized 4c–2e  $\pi$ -bonds in **1**, **3**, and **5** possess high negative  $NICS(0)_{\pi_{zz}}$  values between  $-17$ – $(-25)$  ppm at their geometrical centers (a in **1**, b in **3** and d and f in **5**), indicating the existence of local ring current and  $\pi$ -aromaticity in these regions. Interestingly, the rhombuses covered by delocalized 4c–2e  $\sigma$  bonds also have negative  $NICS(0)_{\sigma}$  values between  $-6$ – $(-7)$  ppm at their centers (c in **3** and e in **5**), evidencing the formation of local  $\sigma$ -aromaticity in these intervals between two  $\pi$ -aromatic rhombuses, well in agreement with AdNDP analyses presented above. Thus, corresponding to the delocalized  $\pi$ - and  $\sigma$ -bond alternations shown in Table 1 in both AdNDP and ALF, these DC planar conjugated borenes possess  $\pi$ - and  $\sigma$ -aromaticity alternations in magnetic properties (NICS criteria).

The analyses presented above indicate that the  $4n + 2$  aromaticity rule originally obtained from monocyclic organic molecules can not be applied to interpret the net aromaticity/antiaromaticity of these DC planar conjugated borene clusters which have multiple aromatic systems. Such unique bonding patterns can only exist in boron-based inorganic clusters in triangular or mixed motifs which possess extensive bond delocalizations to overcome the electron deficiency of the systems.<sup>13–18,21</sup>

### 3 Electron detachment energies

PES in combination with *ab initio* calculations has proven to be a powerful approach in characterizing various gas-phase clusters.<sup>10,21,35–38</sup> We predict in this work the vertical detachment energies (VDEs) of the ground-state DC planar  $B_nH_2^-$  monoanions ( $n = 3, 4, 5, 6, 7, 8, 9$ , and 11) at TDDFT and simulated their PES spectra in Fig. 5. The electronic binding energies of these clusters well fall within the energy range of conventional excitation lasers (0–7 eV) in PES measurements.<sup>35–38</sup> Among these anionic clusters,  $C_{2v}B_{11}H_{12}^-$ ,  $C_2B_9H_{10}^-$ , and  $C_{2v}B_7H_8^-$  have the highest first VDE values of 3.80, 3.03, and 3.40 eV and  $C_2B_9H_{10}^-$ ,  $C_{2h}B_8H_8^-$ , and  $C_2B_5H_6^-$  possesses the largest A–X gaps of 1.67, 1.36, and 1.31 eV between the first peak (X) and the second peak (A), respectively. The high-lying excited states of the  $B_nH_2^-$  neutrals appear to be closely located in energy in many cases and are expected to overlap to a certain degree in the PES measurements.

To elucidate the validity of our theoretical prediction, we compare the simulated PES spectrum of  $C_{2v}B_7H_8^-$  with the available PES spectrum of  $C_{2v}B_7Au_2^-$ .<sup>10,21</sup> Interestingly, the vertical detachment energies of the two isovalent species agree surprisingly well: the first three vertical detachment energies of VDE = 3.40, 4.24 and 4.37 eV calculated for  $C_{2v}B_7H_8^-$  correspond well to the first three PES peaks at 3.52, 4.27, and 4.38 eV observed for  $C_{2v}B_7Au_2^-$ ,<sup>10,21</sup> respectively, strongly supporting the H/Au isolobal analogy. Such a comparison may be extended to other  $B_nX_2^-$  species (X = H, Au, BO) when measured PES spectra are available. We believe that the simulated PES spectra shown in Fig. 5 will well facilitate future PES characterizations of these DC planar monoanions and related species.

We also calculated the ionization potentials (IPs) and electron affinities (EAs) of the most concerned neutrals to facilitate their future spectroscopic investigations. For  $D_{2h}B_4H_2(1)$ ,

$C_{2h} B_6H_2(9)$ ,  $C_{2h} B_8H_2(3)$ , and  $C_{2h} B_{12}H_2(5)$ , IP = 9.42, 9.10, 9.12, and 8.52 eV and EA = 2.25, 2.69, 2.31, and 2.73 eV at B3LYP/6-311+G(d,p) level, respectively.

#### IV. Summary

We have presented in this work a comprehensive first-principles investigation on the conjugated aromatic DC planar  $D_{2h} B_4H_2$ ,  $C_{2h} B_8H_2$ , and  $C_{2h} B_{12}H_2$  which turn out to be the borene analogues of ethylene  $C_2H_4$ , 1,3-butadiene  $C_4H_6$ , and 1,3,5-hexatriene  $C_6H_8$ , respectively. Our results indicate that a  $B_4$  rhombus in DC planar  $B_{2n}H_2$  borenes ( $n = 2, 4, 6$ ) is equivalent to a C=C double-bond unit in the well-known  $C_nH_{n+2}$  conjugated hydrocarbons, expanding the analogous relationship between the dual spaces of hydroborons and hydrocarbons to one dimensional DC planar structures. Such DC planar substructures may be used as precursors to form the double-ring tubular (DR)  $B_{20}$ ,<sup>21</sup> DR-interwoven  $B_{80}$  fullerene,<sup>22</sup> and the DC-interwoven  $\alpha$ -sheet.<sup>23</sup> For example, a DR tubular  $B_{20}$  cluster can be formed by elimination of one  $H_2$  molecule through cyclization of a DC planar  $B_{20}H_2$ . Besides, the  $-H$  terminals in the ground state DC planar  $B_nH_2^{0/-}$  can be partially or completely substituted with  $-Au$  or  $-BO$  radicals to form DC planar  $B_nAu_2^{0/-}$  boron aurides or  $B_n(BO)_2^{0/-}$  boron boronyls.<sup>10,21,38</sup> Syntheses and characterizations of such neutral or anionic species in gaseous phases are highly possible through laser ablation of pure boron or boron-based targets in a hydrogen- or oxygen-seeded atmosphere followed by PES measurements in gaseous phases or IR measurements in isolated matrixes.

#### Acknowledgements

This work was jointly supported by the National Science Foundation of China (No. 20873117 and 21003086) and Shanxi Natural Science Foundation (No. 2010011012-3). The authors sincerely thank Professor Jun Li at Tsinghua University and Prof. Zhi-Xiang Wang at the Graduate University of Chinese Academy of Sciences for inspirational discussions on the project.

#### References

- M. A. Vincent and H. F. Schaefer, *J. Am. Chem. Soc.*, 1981, **103**, 5677.
- S. X. Tian, *J. Phys. Chem. A*, 2005, **109**, 5471.
- A. Ricca and C. W. Bauschlicher, *J. Chem. Phys.*, 1997, **106**, 2317.
- L. A. Curtiss and J. A. Pople, *J. Chem. Phys.*, 1989, **91**, 4809.
- J. F. Dias, G. Rasul, P. R. Seidl, G. K. Surya Prakash and G. A. Olah, *J. Phys. Chem. A*, 2003, **107**, 7981.
- M. L. McKee, Z. X. Wang and P. v. R. Schleyer, *J. Am. Chem. Soc.*, 2000, **122**, 4781.
- P. v. R. Schleyer, G. Subramanian and A. Dransfeld, *J. Am. Chem. Soc.*, 1996, **118**, 9988.
- A. Goursot, E. Pénigault, H. Chermette and J. G. Fripiat, *Can. J. Chem.*, 1986, **64**, 1752.
- (a) J. K. Olson and A. I. Boldyrev, *Inorg. Chem.*, 2009, **48**, 10060; (b) J. K. Olson and A. I. Boldyrev, *Comput. Theor. Chem.*, 2011, **967**, 1; (c) J. K. Olson and A. I. Boldyrev, *Chem. Phys. Lett.*, 2012, **523**, 83; (d) J. K. Olson and A. I. Boldyrev, *Chem. Phys. Lett.*, 2011, **517**, 62.
- H.-J. Zhai and L.-S. Wang, *J. Phys. Chem. A*, 2006, **110**, 1689.
- A. N. Alexandrova, E. Koyle and A. I. Boldyrev, *J. Mol. Model.*, 2005, **12**, 569.
- N. G. Szwacki, V. Weber and C. J. Tymczak, *Nanoscale Res. Lett.*, 2009, **4**, 1085.
- Q. Chen, H. Bai, J.-C. Guo, C.-Q. Miao and S.-D. Li, *Phys. Chem. Chem. Phys.*, 2011, **13**, 20620.
- D.-Z. Li, H.-G. Lu and S.-D. Li, *J. Mol. Model.*, 2012, DOI: 10.1007/s00894-011-1322-y.
- M. Boyukata, C. Ozdogan and Z. B. Guvenc, *J. Mol. Struct. (THEOCHEM)*, 2007, **805**, 91.
- Q. Chen and S.-D. Li, *J. Cluster Sci.*, 2011, **22**, 513.
- H. Bai and S.-D. Li, *J. Cluster Sci.*, 2011, **22**, 525.
- (a) D. Y. Zubarev and A. I. Boldyrev, *Phys. Chem. Chem. Phys.*, 2008, **10**, 5207; (b) D. Y. Zubarev and A. I. Boldyrev, *J. Org. Chem.*, 2008, **73**, 9251; (c) D. Y. Zubarev and A. I. Boldyrev, *J. Phys. Chem. A*, 2009, **113**, 866; (d) T. R. Galeev, Q. Chen, J.-C. Guo, H. Bai, C.-Q. Miao, H.-G. Lu, A. P. Sergeeva, S.-D. Li and A. I. Boldyrev, *Phys. Chem. Chem. Phys.*, 2011, **13**, 11575.
- B. Silvi and A. Savin, *Nature*, 1994, **371**, 683.
- (a) P. v. R. Schleyer, C. Maerker, A. Dransfeld, H.-J. Jiao and N. J. R. E. Hommes, *J. Am. Chem. Soc.*, 1996, **118**, 6317; (b) P. v. R. Schleyer, H. Jiao, N. J. R. v. E. Hommes, V. G. Malkin and O. Malkina, *J. Am. Chem. Soc.*, 1997, **119**, 12669.
- A. N. Alexandrova, A. I. Boldyrev, H.-J. Zhai and L.-S. Wang, *Coord. Chem. Rev.*, 2006, **250**, 2811.
- N. G. Szwacki, A. Sadrzadeh and B. I. Yakobson, *Phys. Rev. Lett.*, 2007, **98**, 166804.
- H. Tang and S. Ismail-Beigi, *Phys. Rev. Lett.*, 2007, **99**, 115501.
- A. D. Beck, *J. Chem. Phys.*, 1993, **98**, 5648.
- C. Lee, W. Yang and R. G. Parr, *Phys. Rev. B*, 1988, **37**, 785.
- M. J. Frisch, G. W. Trucks, H. B. Schlegel, G. E. Scuseria, M. A. Robb, J. R. Cheeseman, J. A. Montgomery, Jr., T. Vreven, K. N. Kudin, J. C. Burant, J. M. Millam, S. S. Iyengar, J. Tomasi, V. Barone, B. Mennucci, M. Cossi, G. Scalmani, N. Rega, G. A. Petersson, H. Nakatsuji, M. Hada, M. Ehara, K. Toyota, R. Fukuda, J. Hasegawa, M. Ishida, T. Nakajima, Y. Honda, O. Kitao, H. Nakai, M. Klene, X. Li, J. E. Knox, H. P. Hratchian, J. B. Cross, V. Bakken, C. Adamo, J. Jaramillo, R. Gomperts, R. E. Stratmann, O. Yazyev, A. J. Austin, R. Cammi, C. Pomelli, J. Ochterski, P. Y. Ayala, K. Morokuma, G. A. Voth, P. Salvador, J. J. Dannenberg, V. G. Zakrzewski, S. Dapprich, A. D. Daniels, M. C. Strain, O. Farkas, D. K. Malick, A. D. Rabuck, K. Raghavachari, J. B. Foresman, J. V. Ortiz, Q. Cui, A. G. Baboul, S. Clifford, J. Cioslowski, B. B. Stefanov, G. Liu, A. Liashenko, P. Piskorz, I. Komaromi, R. L. Martin, D. J. Fox, T. Keith, M. A. Al-Laham, C. Y. Peng, A. Nanayakkara, M. Challacombe, P. M. W. Gill, B. G. Johnson, W. Chen, M. W. Wong, C. Gonzalez and J. A. Pople, *GAUSSIAN03 (Revision A.01)*, Gaussian, Inc., Wallingford, CT, 2004.
- A. N. Alexandrova, A. I. Boldyrev, Y.-J. Fu, X.-B. Wang and L.-S. Wang, *J. Chem. Phys.*, 2004, **121**, 5709.
- A. N. Alexandrova and A. I. Boldyrev, *J. Chem. Theory Comput.*, 2005, **1**, 566.
- (a) J. A. Pople, M. Head-Gordon and K. Raghavachari, *J. Chem. Phys.*, 1987, **87**, 5968; (b) G. E. Scuseria and H. F. Schaefer III, *J. Chem. Phys.*, 1989, **90**, 3700; (c) G. E. Scuseria, C. L. Janssen and H. F. Schaefer III, *J. Chem. Phys.*, 1988, **89**, 7382; (d) J. Cizek, *Adv. Chem. Phys.*, 1969, **14**, 35.
- A. Becke and K. Edgecombe, *J. Chem. Phys.*, 1990, **92**, 5397.
- S. Portmann, *Molekel, Version 4.3*, Swiss National Supercomputing Centre/Swiss Federal Institute of Technology, Zurich, 2002.
- (a) A. E. Reed, L. A. Curtiss and F. Weinhold, *Chem. Rev.*, 1988, **88**, 899; (b) F. Weinhold and C. R. Landis, in *Valency and Bonding: A Natural Bond Orbital Donor-Acceptor Perspective*, Cambridge University Press, New York, 2003.
- (a) M. E. Casida, C. Jamorski, K. C. Casida and D. R. Salahub, *J. Chem. Phys.*, 1998, **108**, 4439; (b) R. Bauernschmitt and R. Ahlrichs, *Chem. Phys. Lett.*, 1996, **256**, 454.
- J. C. Santos, J. Andres, A. Aizman and P. Fuentealba, *J. Chem. Theory Comput.*, 2005, **1**, 83.
- A. P. Sergeeva, D. Y. Zubarev, H.-J. Zhai, A. I. Boldyrev and L.-S. Wang, *J. Am. Chem. Soc.*, 2008, **130**, 7244.
- W. Huang, A. P. Sergeeva, H.-J. Zhai, B. B. Averkiev, L.-S. Wang and A. I. Boldyrev, *Nat. Chem.*, 2010, **2**, 202.
- A. P. Sergeeva, B. B. Averkiev, H.-J. Zhai, A. I. Boldyrev and L.-S. Wang, *J. Chem. Phys.*, 2011, **134**, 224304.
- (a) H.-J. Zhai, S.-D. Li and L.-S. Wang, *J. Phys. Chem. A*, 2007, **111**, 1030; (b) H. J. Zhai, S.-D. Li and L.-S. Wang, *J. Am. Chem. Soc.*, 2007, **129**, 9254; (c) S.-D. Li, H.-J. Zhai and L.-S. Wang, *J. Am. Chem. Soc.*, 2008, **130**, 2573.